Flood susceptibility assessment using machine learning approach in the Mohana-Khutiya River of Nepal

Menuka Maharjan [a,b,*], Sachin Timilsina [c], Santosh Ayer [d], Bikram Singh [b], Bikram Manandhar [b], Amir Sedhain [b]

[a] School of Forestry and Natural Resource Management, Institute of Forestry, Tribhuvan University, 44600, Kathmandu, Nepal
[b] Tribhuvan University, Institute of Forestry, Hetauda Campus, 44107, Makwanpur, Nepal
[c] Tribhuvan University, Institute of Forestry, Pokhara Campus, 33700, Pokhara, Nepal
[d] Agriculture and Forestry University, College of Natural Resource Management (CNRM), 56310, Katari, Nepal

ARTICLE INFO

ABSTRACT

Nepal, known for its challenging topography and fragile geology is confronted with the constant threat of floods leading to substantial socio-economic losses annually. However, the country's efforts in planning and managing flood risks remain insufficient, especially in the vulnerable Mohana-Khutiya River. Therefore, this study focused on the Mohana-Khutiya River and utilizes the Maximum Entropy (MaxEnt) model to comprehensively map flood susceptibility and fill crucial gaps in flood risk assessments. This study employed a combination of 10 geospatial environmental layers and field-based past flood inventory to implement the MaxEnt machine learning model for flood susceptibility modeling. The available past flood data were divided into two sets, with 75% allocated for model construction and the remaining 25% for model validation. This study demonstrated that the proximity of the river had a significant impact (33.1%) on the occurrence of the flood. Surprisingly, the amount of annual precipitation throughout the year exhibited no detectable contribution to the flood event in the study site. About 4.9% area came under the high flood susceptible zone followed by 12.75 % in the moderate zone and 82.34% in the low-risk zone. The model exhibited excellent performance with an Area Under Curve (AUC) value of 0.935 and a low standard deviation of 0.018, indicating accurate predictions and consistent precision. These results highlight the model's reliability and its significance for developing disaster management policy by local government in the study site. Future research should refine the MaxEnt model by including more variables, validating against observed flood events, and exploring integration with other flood modeling approaches.

1. Introduction

Floods are highly prevalent and catastrophic natural phenomenon that occurs on a global scale (Ghapar et al., 2018; Glago, 2021). In 2019, approximately 24.9 million new displacements were recorded globally, with nearly three-quarters attributed to disasters. Weather-related hazards, specifically floods, accounted for over 95 % of these displacements, amounting to around 10 million people affected (IDMC, 2020). Floods triggered 2.7 million internal displacements across the world, significantly fewer than the 5.3 million recorded in 2021 (IDMC, 2023). Flood is described as a natural calamity that arises from the excessive accumulation of water in an area, typically caused by heavy rainfall, snowmelt, river overflow, or other factors (Barredo, 2007; Sivakumar, 2015). It is classified based on various criteria, including their source (riverine,

coastal, flash floods), location (localized, urban, rural), severity or recurrence interval (normal, severe, catastrophic floods), duration (short-term, long-term floods), impact (minor, moderate, major floods), and geological setting (fluvial, pluvial, coastal floods) (Glago, 2021).

Floods can have significant socio-economic impacts including damage or destruction of property, displacement of communities, posing risks to human lives and health, as well as adverse effects on ecosystems and natural resources such as soil erosion, sedimentation, and water pollution (Glago, 2021). However, it's important to note that floods can also have positive impacts, such as contributing to the replenishment of water resources, enriching soil fertility through sedimentation, and creating or restoring habitats for various plants and animals (Aldardasawi and Eren, 2021).

Approximately 23% (equivalent to 1.81 billion individuals) of the

global population is at risk of being directly impacted by flooding that has a depth of over 0.15 m (Rentschler et al., 2022). About 89% of the global population vulnerable to floods resides in developing countries (Rentschler et al., 2022). In Sub-Saharan Africa, 44% of the 170 million people are in extreme poverty (less than $1.90 per day) and face significant flood risk (Rentschler et al., 2022). While subsisting on less than $5.5 per day, at least 780 million people live in areas in high danger of flooding (Rentschler et al., 2022). In 2021, there were 206 major flood disasters worldwide, causing over 4393 deaths and affecting 29.2 million people. These flood disasters resulted in direct economic losses exceeding USD 74.6 billion, accounting for about 30% of total disaster economic losses (Global Natural Disaster Assessment Report, 2022). In Western Europe in 2021, more than 180 people died, over 750 were injured, and many suffered financially (Lehmkuhl et al., 2022). Conversely, roughly 243 individuals perished in European countries like Germany, Belgium, Romania, Italy, and Austria because of flooding (European floods, 2021). In West and Central Africa in 2021, flooding impacted 1.4 million individuals spanning 15 nations, resulting in 305 deaths, thousands of injuries, and the displacement of nearly 378,000 individuals (OCHA, 2022). Similarly, in 2022, flooding in New South Wales and Queensland, Australia, claimed 26 lives, damaged thousands of homes, and led to billions in insurance claims (AIDR, 2022).

Comparatively South Asian countries are highly vulnerable to flooding and its consequences. Over 1.24 billion people reside in flood-prone areas, notably China (395 million individuals) and India (390 million individuals) collectively representing almost a quarter of the global population (Rentschler et al., 2022). Countries like India, China, Bangladesh, and Pakistan have grappled with flood risks for decades (ADPC, 2005; Kazi, 2014; Abbas et al., 2016). India, Nepal, and Bangladesh are linked due to the flood effect, which killed 1200 people and affected 41 million people in Southern Nepal, Northern India, and Bangladesh (IFRC, 2020). Additionally, in July 2021, flooding in China claimed the lives of 398 people (Ye, 2022). For instance, Pakistan experienced widespread flooding, affecting 33 million people and resulting in over 1700 deaths as of November 2022 (UNICEF, 2022). In India's Assam state, floods impacted 5.6 million people, displacing 4.7 million, damaging 108,308 ha of crops, and affecting millions of animals in 2022 (Juned, 2022). Similarly, in China's Henan province, a devastating flood claimed hundreds of lives in July 2021 (Ye, 2022). Compared to the average for the last 30 years, the frequency of flood disasters increased by 48% globally in 2021, however the number of fatalities was 35% less, and the count of affected individuals was 71% less (Global Natural Disaster Assessment Report, 2022).

Due to rugged topography, concentrated monsoon rains, fragile geology, and unsustainable land management, Nepal is also highly susceptible to devastating floods with a recorded 4160 floods from 1971 to 2016 resulting in casualties and infrastructure damage (Shrestha et al., 2022). Each year, floods in Nepal lead to an average of 175 fatalities and cause economic losses that surpass USD 140 million (ADB, 2019). Nepal ranks tenth globally in terms of physical exposure to fluvial flooding (ADB, 2019). A total of 4160 floods were documented between 1971 and 2016, leading to both human casualties and significant damage to infrastructure in Nepal (Shrestha et al., 2022). Floods in Nepal between 1954 and 2018 resulted in 7599 fatalities, 6.1 million impacted, and 10.6 billion USD in losses to the economy (EmDAT, 2019). In 2017, 179 people died, more than 75 people were injured, 42 individuals remain missing, and the impact extended to 15,303 households (Sharma et al., 2019).

In August 2017, major flooding affected around 1.7 million people in Nepal, resulting in at least 140 deaths and 80% of the Terai region being flooded (UNICEF, 2017). The damage was estimated to cost the government USD 584.7 million, with an additional USD 375.8 Million required for housing reconstruction alone (NPC, 2017). According to historical records, Nepal had significant flooding in the Tinao, Koshi, Tadi, and Sunkoshis basins in the years 1978, 1980, 1985, and 1987 respectively that took the lives of 1336 individuals (Ghatak et al., 2012;

Kafle et al., 2017). In October 2021, Nepal faced a 15% excess in monsoon rainfall, resulting in substantial agricultural losses, including the destruction of rice crops worth around 26 billion Nepalese rupees, along with associated human and property casualties (OCHA, 2021; MoAD, 2021). Therefore, Nepal's vulnerability to floods is a serious concern due to its high susceptibility to seasonal monsoon floods which needs to be addressed to minimize potential casualties and property damage (Dewan, 2015).

Flood susceptibility mapping (FSM) has been employed to detect and characterize areas at elevated risk of flooding based on their physical attributes (Vojtek and Vojteková, 2019). These maps play a pivotal role in minimizing flood-related damages, a critical aspect of disaster mitigation efforts (Sahoo and Sreeja, 2015). The identification of regions prone to flooding involves the consideration of factors like topography, land use, soil types, and hydrological features (Lee and Kim, 2021). The primary objective is to facilitate targeted measures that decrease the likelihood of flooding, thereby reducing associated damages and contributing to the overall reduction of disaster risks (Rosmadi et al., 2023). Furthermore, these maps are instrumental in developing early warning systems, and enhancing the readiness and response capabilities of communities located in high-risk areas (Bajracharya et al., 2021). Therefore, various traditional methods for FSM have been used previously in Nepal (Banstola et al., 2019; Dhakal, 2020; Karki and Khadka, 2020; Karna et al., 2021; Paudel et al., 2019; Regmi, 2021; Sangroula et al., 2022; Shrestha et al., 2022).

These studies have primarily relied on physical process-based models, such as hydrological models like Hydrologic Engineering Center's Hydrologic Modeling System (HEC-HMS) (Karna et al., 2021; Paudel et al., 2019; Sangroula et al., 2022), Hydrologic Engineering Center's River Analysis System (HEC-RAS) (Banstola et al., 2019; Dhakal, 2020; Regmi, 2021; Shrestha et al., 2022), Soil and Water Assessment Tool (SWAT) model (Karki and Khadka, 2020), as well as statistical methods that fit probability distribution functions to annual maximum values (Brunner et al., 2021). Nonetheless, each of these methodologies comes with its set of constraints. For instance, physically based models and numerical models depend upon various hydro-geomorphological observation data (Antwi-Agyakwa et al., 2023; Khosravi et al., 2016a; Mosavi et al., 2018). Additionally, challenges arising from issues of data reliability and accessibility due to the nature of the terrain, climate, or other factors in physically based and numerical modeling can significantly impact the accuracy and applicability of these models (Khosravi et al., 2016a; Seydi et al., 2022). Furthermore, computational complexities and parameter selection in physically based models are also hurdles affecting the reliability and accuracy of the model outputs (Fu et al., 2020).

In recent years, the increasing popularity of employing multi-criteria decision-making methods in FSM is evident. However, the reliance on expert judgment in these methods introduces biases, and even minor adjustments in parameter weights can significantly influence the outcomes (de Brito et al., 2019; Ali et al., 2020; Mehravar et al., 2023). Conversely, widely used statistical methods like frequency ratio (Tehrany et al., 2014, 2017) and logistic regression models are prevalent in flood modeling but are constrained by linear assumptions, potentially overlooking the non-linear behavior of floods (Sharma et al., 2019; Khosravi et al., 2016a; Andaryani et al., 2021). While hydrological/hydraulic-based models leverage non-linearity, their accuracy may be influenced by geomorphological and environmental factors (Seydi et al., 2022). For basins exceeding 1000 km^2, achieving accurate two or three-dimensional analysis using hydrodynamic models like HECRAS becomes impractical (Khosravi et al., 2016a).

With no prior assumptions or in-depth knowledge of the physical processes, the Machine Learning approach has been developed to overcome the limitations of traditional models for FSM (Mishra et al., 2022). To do this, information based on available data is leveraged. Rapid geographic data analysis is made possible by this machine-learning approach (Dodangeh et al., 2020; Mishra et al., 2022). Artificial neural networks (Andaryani et al., 2021), support vector machines (Li et al.,

2019a,b; Costache et al., 2020; Nachappa et al., 2020), gradient boosting (Ghosh et al., 2022; Seydi et al., 2022), and random forest (Schmidt et al., 2020; Nachappa et al., 2020) are some frequently used machine learning approach in FSM. However, in Nepal, very few studies have been conducted using a machine-learning approach in the realm of flood risk management.

For instance, studies have explored the application of Gaussian process regression and support vector machines in the Koshi Basin (Baig et al., 2022). Similarly, Shreevastav et al. (2022) employed Maximum Entropy (MaxEnt) model in the Southern Bagmati corridor (Sarlahi and Rautahat) to identify flood risk-prone areas as well as model flood susceptibility in a segment of the Bagmati basin. The MaxEnt model offers several advantages that make it well-suited for flood susceptibility assessment in areas with limited hydraulic and hydrological data (Shreevastav et al., 2022). One key advantage is its ability to make predictions based solely on the presence of past flood events, eliminating the need for extensive stream flow observations for calibration and validation (Phillips et al., 2006; Zeng et al., 2021). This is particularly valuable in situations where such data may be scarce or contain gaps, as is often the case in developing countries like Nepal (Skilodimou et al., 2019; Jehanzaib et al., 2022). Furthermore, the MaxEnt model is capable of integrating external data sources, such as satellite imagery, to estimate crucial environmental variables like precipitation and temperature (Zeng et al., 2021). This is a crucial feature in areas where direct measurements of these variables may not be readily available (Zeng et al., 2021). In this context, the MaxEnt model emerges as the best alternative for flood susceptibility modeling research.

Mohana-Khutiya River of Nepal is particularly vulnerable to flood and erosion hazards due to its steep slopes (average 25.3°) and unstable geological structure in the Siwalik, combined with the flat and vulnerable floodplain zone in the south (Marsh, 2020). Additionally, the lack of forest cover in the bank corridor increases the risk of stream bank erosion, which might result in land loss and property damage (Marsh, 2020). Despite the high risk of flooding in the region, there are inadequate flood risk assessments that can guide local authorities and communities in disaster preparedness and management. The local government and disaster management authorities play a critical role in safeguarding communities against the impacts of floods (Shah et al., 2019). By providing a detailed and accurate flood susceptibility map for the Mohana-Khutiya River, this research offers invaluable support to local government agencies in enhancing their disaster management plans. The utilization of a machine learning approach ensures a cost-effective and efficient means of generating these maps (Shreevastav et al., 2022), proving especially advantageous in regions with limited data availability like the Mohana-Khutiya River.

The significance of this research extends to its potential impact on resource allocation and prioritization within disaster management strategies in the Mohana-Khutiya River. By harnessing advanced technology to create accurate flood susceptibility maps, local authorities can optimize their preparedness and response efforts, ultimately leading to more effective risk mitigation and reduced socio-economic losses (Parajuli et al., 2023). Therefore, our study further extends the application of the MaxEnt model to predict flood susceptibility (Shreevastav et al., 2022) in the Mohana-Khutiya River of Nepal. By expanding the application of this model, we aim to deepen our understanding of flood risk dynamics, pinpoint high-susceptibility zones, and establish tailored approaches to alleviate floods and manage disasters within the Mohana-Khutiya River area of Nepal. We also aim to contribute to an advanced understanding of the innovative MaxEnt model's applicability in different geographical contexts within Nepal.

2. Methodology

2.1. Study site

The current research took place within the Mohana-Khutiya River

area (Fig. 1), positioned between the Siwalik Ranges and the Terai region (Marsh, 2020). The Siwalik Ranges represent the youngest mountain range in the Himalayan orogeny, and they stand out as one of the most dynamically active zones within the Himalayas (Upreti, 1999; Stöcklin, 2008). The geological dynamics in this area, including rock deformation, dislocation, and uplift, have resulted in an intricate geological configuration and an unstable landscape prone to erosion (Nakata, 1989; Lavé and Avouac, 2001). The climate of the study site is tropical. Due to the Mohana-Khutiya River's high susceptibility to flooding, over the years, floods have claimed lives, damaged homes, and other buildings, disrupted public infrastructures, and destroyed agricultural land and harvests.

The riverbanks of the Mohana River system are very fragile and prone to erosion and some of its areas are even flattened due to flooding. With heightened rainfall intensity, river discharge increases to such an extent that the incidence of flood events escalates, resulting in property damage throughout the rainy season (Marsh, 2020). This river experienced 390 floods between 1991 and 2015, of which 35 caused economic losses of at least NRs 1 million, 37 resulted in a total of 440 fatalities, and 79 resulted in the destruction of more than 10 dwellings (ADB, 2020). In October 2021 and 2022, unseasonal rain caused flooding and destroyed harvest-ready paddy crops in Kailali and Kanchanpur (Fig. 2) (The Kathmandu Post, 2021; The Himalayan, 2022; Beshir et al., 2022). Anticipated increases in population and resource development within flood-prone zones of the Terai Region are expected to elevate the likelihood of flooding. This risk will be made worse by climate change (Marsh, 2020).

Hence, the Mohana-Khutiya River is identified as a priority River for Flood Risk Management by the Ministry of Energy, Water Resources and Irrigation of Nepal to manage the flows through rivers to reduce the incidence of severe floods and provide protection to people, houses, public infrastructure, and agricultural land.

2.2. Data used

2.2.1. Inventory of flood history and environmental variables

A total of 45 flood occurrence data were collected from the study site. From this collection of flood occurrence locations, a training group consisting of 34 flood locations, or 75%, and a validation group consisting of 11 flood locations, or 25%, was created. Total 10 environmental parameters i.e., Annual temperature, Soil type, Annual precipitation, Land Use Land Cover Change (LULC), Topographic Wetness Index (TWI), River distance, Digital Elevation Model (DEM), Normalized Difference Vegetation Index (NDVI), Drainage density and Slope were utilized for flood forecasting using MaxEnt model (Table 1).

2.2.2. Multicollinearity analysis

Before running the mode, the correlation was run among the environment layer (independent layer). To prevent the multicollinearity impact and improve model performance, one variable is deleted if the correlation between the two variables is more than 0.8.

To finish this method, field data from several flooding events that had happened in the study area were verified using the Area Under the Curve (AUC) method (Fig. 3).

3. Results

3.1. Flood susceptibility mapping of the study area

Flood susceptibility was categorized into three zones i.e., High (Red color), Moderate (Yellow color), and Low (Blue color) (Fig. 4). About 4.9% area came under the high flood susceptibility zone followed by 12.75 % in the moderate zone and 82.34% in low susceptibility zone (Table 2).
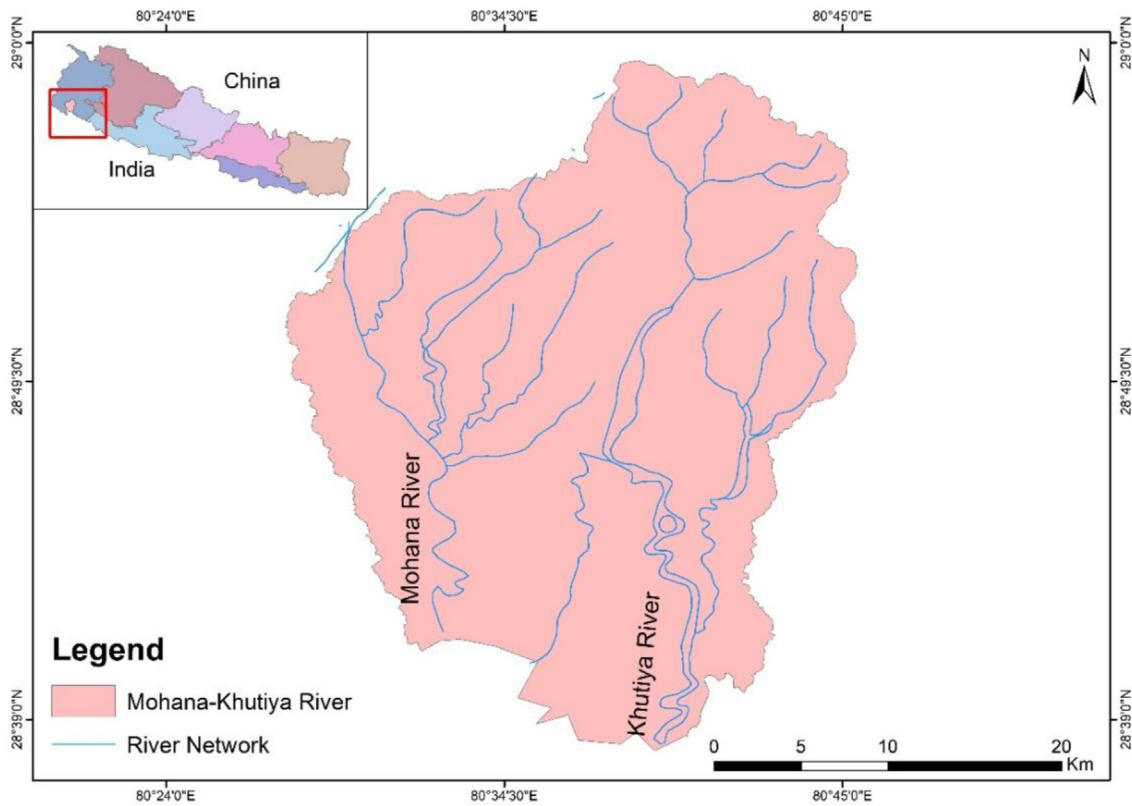
Fig. 1. Map of the study site showing the Mohana-Khutiya River.

Fig. 2. Flood events at the study site on July 19, 2022 (Photo credit: Dependra Singh, 2022).

3.2. *Flood susceptibility assessment of village*

A flood susceptibility assessment of villages was conducted, and villages were categorized into three groups i.e. high susceptible villages (dark red color circle), moderately susceptible villages (orange color circle), and low susceptible villages (green color circle) (Fig. 5). Altogether, there are 20 villages in the high susceptible zone, 46 in the moderate susceptible zone and 105 in the low susceptible zone (Table 3).

3.3. *Response of environmental variables to a flood event*

The distance from the river contributes higher (33.1%) than others followed by LULC, DEM, Drainage density, Soil type, Annual temperature, TWI, Slope, NDVI, and Annual precipitation (Table 4). Among 10 environmental variables, annual precipitation was the least significant for flood susceptibility modeling in this study area.

Table 1

Data accessibility for environmental variables (Adapted from Shreevastav et al., 2022).

S.N.	Environment variables	Availability from/source	Resolution normalized
1	LULC	ArcGIS online(https://livingatlas.arcgis.com/landcover/)	10m × 10m
2	Annual precipitation	World Clim(https://www.worldclim.org/data/bioclim.html)	10m × 10m
3	Annual temperature	World Clim(https://www.worldclim.org/data/bioclim.html)	10m × 10m
4	Soil type	ICIMOD(https://rds.icimod.org/home/datadetail?metadataid=1889)	10m × 10m
5	NDVI	Sentinel-2(https://dataspace.copernicus.eu/explore-data/data-collections)	10m × 10m
6	River distance	ICIMOD(http://rds.icimod.org/Home/DataDetail?metadataId=2956)	10m × 10m
7	TWI	From DEM(https://earthexplorer.usgs.gov/)	10m × 10m
8	DEM	USGS(https://earthexplorer.usgs.gov/)	10m × 10m
9	Drainage density	From DEM(https://earthexplorer.usgs.gov/)	10m × 10m
10	Slope	From DEM(https://earthexplorer.usgs.gov/)	10m × 10m

3.3.1. Distance from river

There was an inverse relationship between flood susceptibility and distance from the river network, implying that increasing distance reduces the possibility of flooding (Fig. 6).

3.3.2. Land use land cover (LULC)

Flood susceptibility was the highest in shrub/scrub land compared to other LULC (Fig. 7). Among seven LULC classes, the lowest flood susceptibility was found in trees (i.e., Forest).

3.3.3. Digital Elevation Model (DEM)

Similar to Distance from River, there was an inverse relationship between flood susceptibility and elevation i.e., making plain regions the most susceptible to flooding catastrophes, which frequently occur in locations with low topographic elevations or downstream areas (Fig. 8).

3.3.4. Drainage density

Interestingly, drainage density and flood susceptibility demonstrated a positive relationship i.e., flood susceptibility increased with increasing drainage density (Fig. 9).

3.3.5. Soil type

Flood susceptibility was the highest in Haplaquents, Haplaqepts, and Eutrocrepts soil compared to other soil (Fig. 10).

3.3.6. Annual temperature

Till 24 °C there was no substantial link between susceptibility of flooding and annual temperature (Fig. 11). However, the flood risk increased with rising temperature above 24 °C.

3.3.7. Topographic Wetness Index (TWI)

The flood susceptibility was the maximum at TWI value 5 (Fig. 12). Flood risk decreased with increasing TWI (value at 24).

3.3.8. Normalized Difference Vegetation Index (NDVI)

Flood susceptibility was the maximum when the NDVI value was between −0.3 and 0.3 (Fig. 13). However, flood susceptibility decreased after the NDVI value was 0.3.

3.3.9. Annual precipitation

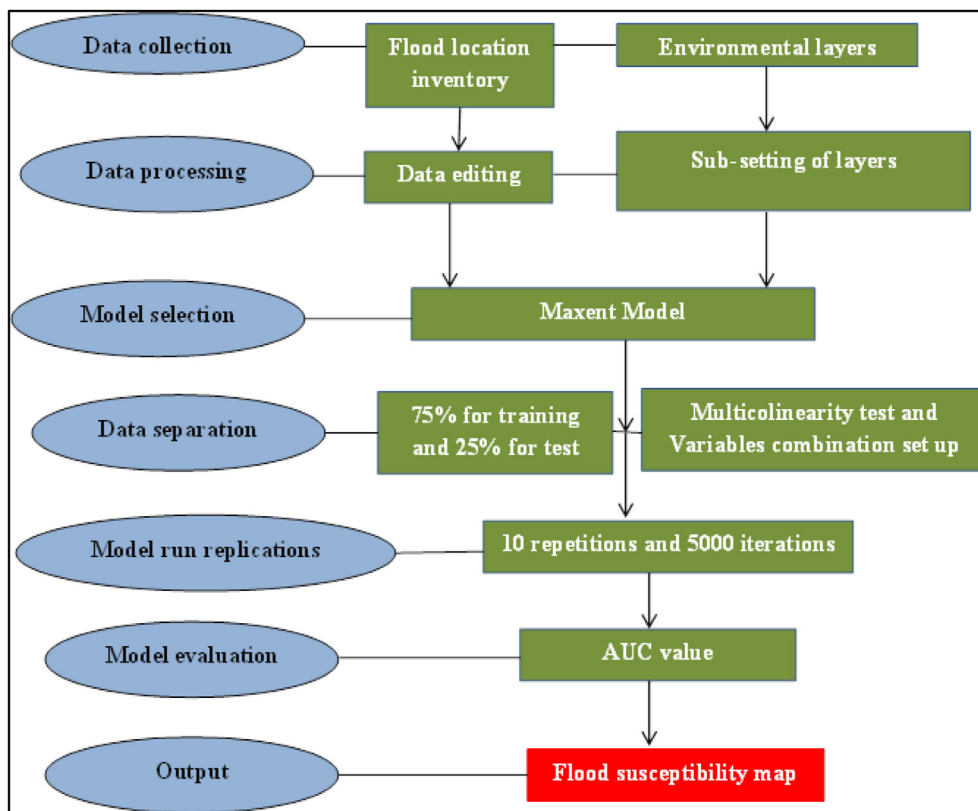Flood susceptibility remains constant up to an annual precipitation of
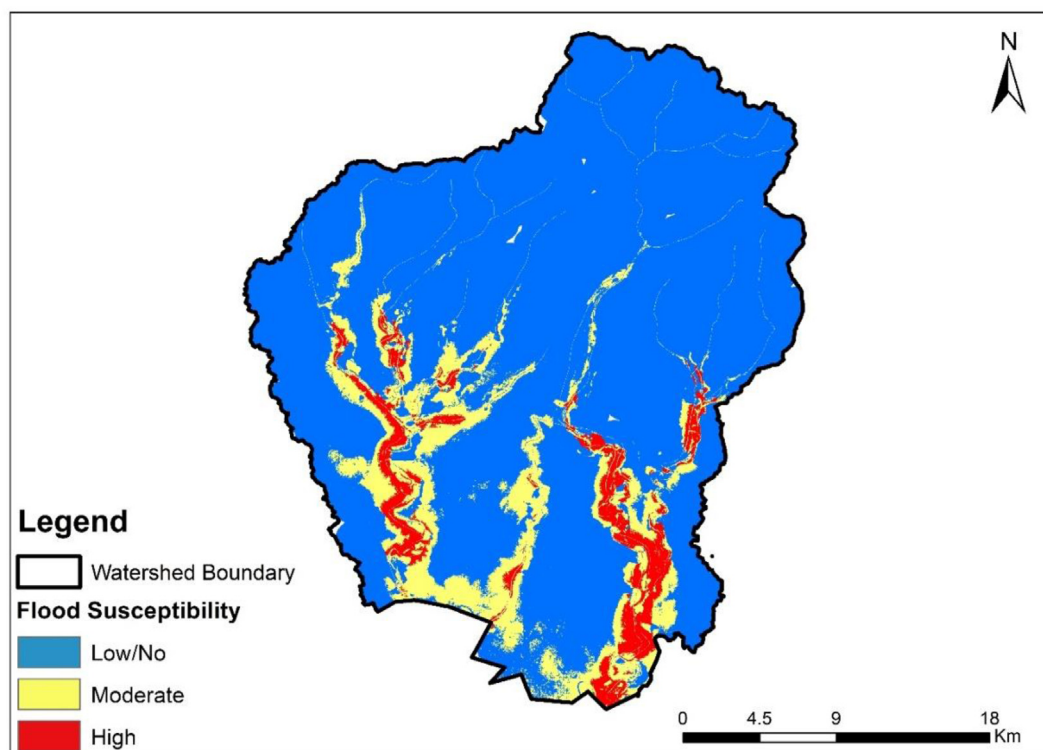

Fig. 3. Methodological flow chart.

Fig. 4. Flood susceptibility mapping of the study area.

1500 mm (Fig. 14). However, flood susceptibility sharply rose from 1500 mm to 1700 mm of annual precipitation. The flood susceptibility declined when annual precipitation was above 1700 mm.

3.4. Performance of MaxEnt model

The calculated Area under Curve (AUC) was 0.935, with a standard deviation of 0.018 (Fig. 15). The AUC values were divided into three ranges: less than 0.5 for not fair, 0.7–0.8 for fair, 0.8–0.899 for good, and above 0.899 for excellent.

4. Discussion

4.1. Flood susceptibility mapping

Through the classification of flood susceptibility into distinct zones, the spatial distribution of susceptibility has been effectively visualized (Fig. 4). The identification of approximately 4.9% of the Mohana-Khutiya River area as high flood susceptible signifies concentrated areas that are at heightened susceptibility of experiencing significant flooding followed by 12.75% as moderate susceptible and 82.34% as low flood susceptible area highlights the varying degrees of vulnerability within the river. Shreevastav et al. (2022) conducted a similar study in the southern Bagmati corridor of Nepal, employing the MaxEnt model which reported that the area under high, moderate, and low flood susceptible was 7.55% 9.48%, and 82.97% respectively. Similarly, at the micro level, the assessment of flood susceptibility for individual villages within the river presents a pivotal perspective on localized vulnerability. This study

found that a total of 20 villages are under the high susceptible zone, 46 within the moderate susceptible zone, and 105 within the low zone (Fig. 5).

In contrast, Shreevastav et al. (2022) observed 41 villages falling within the high-risk zone, 27 villages within the moderate-risk zone, and 123 villages classified as being in the low-risk zone. This divergence can be attributed to the distinct hydrological, geographical, and infrastructural characteristics inherent to the river (Janizadeh et al., 2019; Dung et al., 2022). This finding holds significant implications for disaster preparedness, management, and land-use planning. The high flood-risk areas demand immediate attention due to their risk of severe flooding (Kron, 2005; Erena and Worku, 2018). These regions could benefit from the implementation of robust flood protection measures, including infrastructure improvements and early warning systems (Hallegatte, 2009; Rogers and Tsirkunov, 2011; Perera et al., 2019). Moderate susceptible areas indicate a need for intermediate measures, such as enhanced community awareness and preparedness initiatives, to mitigate potential damages (Abbas et al., 2016; Wang et al., 2022).

The large proportion of low flood susceptible areas provides an opportunity for informed land-use planning that considers the lower vulnerability, promoting sustainable development and reducing exposure to flood hazards (Most and Marchand, 2017). The findings also underscore the importance of targeted resource allocation and interventions. With precise knowledge of where high and moderate susceptible areas are concentrated, resources can be channeled more effectively to areas that need them the most (Munawar et al., 2021). By incorporating this flood risk assessment into decision-making processes, authorities can develop strategic disaster response plans, allocate funds for infrastructure improvements, and prioritize the implementation of measures that enhance community resilience.

4.2. Performance of environment variables in response to a flood event

This study focuses specifically on utilizing the MaxEnt model to conduct flood susceptibility modeling in the Mohan-Khutiya River,
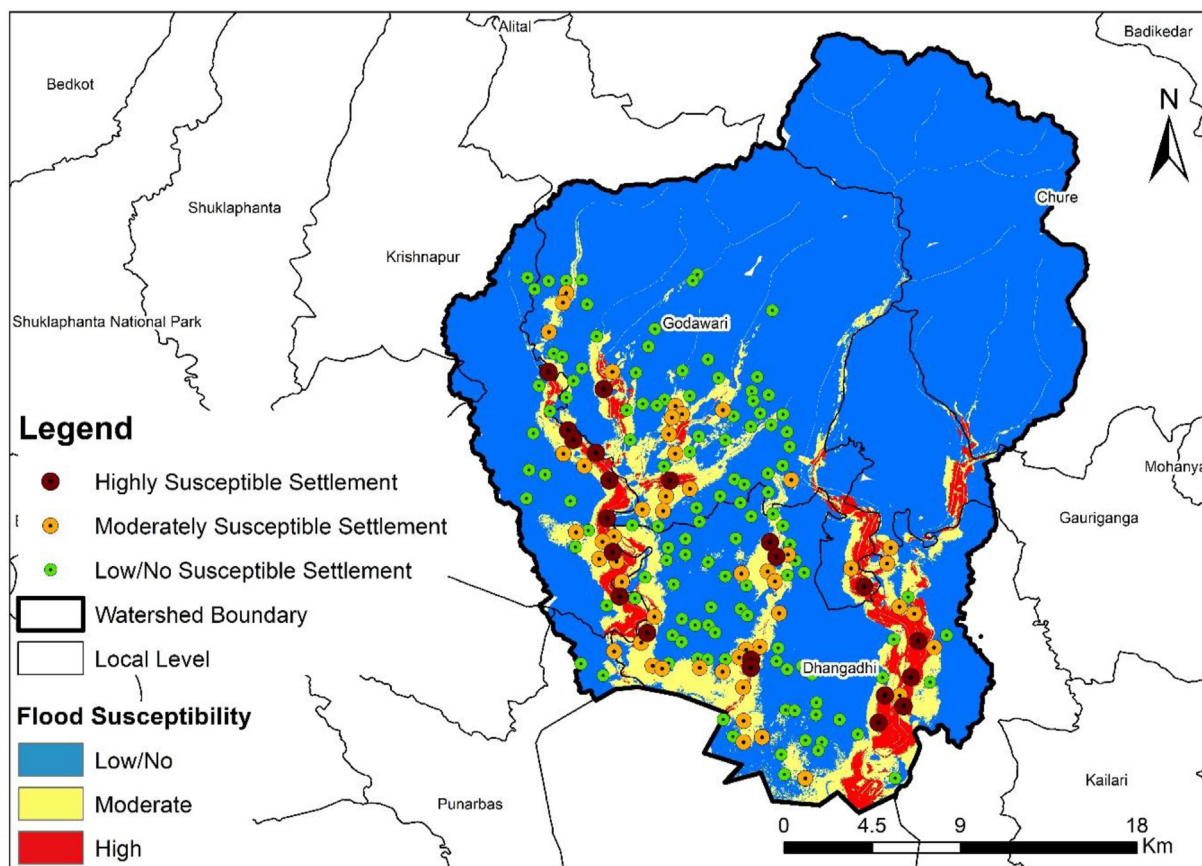
Table 2
Statistics on flood susceptibility.

S. N	Flood susceptibility	Area(km²)	Percentage (%)
1	High	35.40	4.90
2	Moderate	92.09	12.75
3	Low/No	594.61	82.34

Fig. 5. Villages at flood susceptibility.

located in the Kailali and Kanchanpur districts of Nepal (Fig. 1). The flood susceptibility modeling refers to the ease with which each section of the basin is inundated (Hammami et al., 2019; Das, 2019; Das and Gupta, 2021). There is research using the MaxEnt model in the Koshi Basin (Baig et al., 2022) and a part of the Bagmati Basin in Nepal (Shreevastav et al., 2022) using Geographic Information Systems (Ozkan and Tarhan, 2016). To spatially predict flood susceptibility, an advanced machine learning model (MaxEnt) was selected for the following reasons: (1) The MaxEnt model may function with a variety of conditioning factors; (2) it can also depict the non-linear relationship between flood conditioning factors and flood occurrence; and (3) the MaxEnt model doesn't establish strict assumptions before research (Siahkamari et al.,

2018). Additionally, the MaxEnt model is machine learning-based and generates spatial predictions based on limited data for flood hazard zoning (Rahmati et al., 2016a).

Our study found notable correlations between flood inundation occurrences and the proximity to rivers (Tehrany et al., 2014; Papaioannou et al., 2015; Ahmadisharaf et al., 2016). In addition, Eini et al. (2020) in the Gharesoo and Cham-Bashir rivers crossing Kermanshah City, Iran found a high risk of flooding near the riverbanks. The finding emphasizes those certain environmental variables, such as altitude and drainage density (Figs. 8 and 9), had a greater impact on the likelihood of flooding. This finding corresponds with the results reported by Kalyanapu et al. (2012) in Swannanoa River, United States of America (USA), Tehrany

Table 3
Flood-prone villages.

S. N	Villages in flood-prone areas	Name of Villages
1	High	Badhara, Bajhangetol, Barhanambarbasti, Bela, Beli, Chaukidada, Dhanchauri, Dhangadhigaun, Geti, Ghodaghat, Kaluwapur, Karkikatan, Khallamauriphata, Kyampas mod Majgau, Mauriphata, Rajghat, Shantikatan, Shantipur, Tarbariya
2	Moderate	Ailyankatan, Bahuntol, Bandarkhal, Bangragaun, Basantatol, Basantapur(Jhanjhatpur),Bhansar, Bhansarkatan, Chaitanyapur, Chatakpur, Chyakhalakholagaun, Damaura, Devipur, Dhurjanna, Doghara, Gaurikatan, Geta, Ghodaghat, Gholpurwa, Jaligaun, Jugedakatan, Kaluwapur, Kaluwapur (Aghillopatti),Khamaura, Khunatola, Kyampas road, Lalpur (Kolikatan),Mallomatiyari, Margaht, Milanchok, Murkatti, Nahartol, Najariya, Nargidanda, Panchadhaki, Pathari, Pipariya, Rajghat, Saraswatinagar, Setopul, Shantinagar, Shantitol, Shivarampur, Surmikatan, Taratal, Urma
3	Low	A-Gaun, Amarbasti, Attariya, Badeha, Baiyabehadi, Baluwaphata, Bandarpur, Bangesal(Olani),Bankhet, Barbata, Barbatagau, Basantapur (Jhanjhatpur),Baskheda, Baskota, Behandi, Bela, Belikatan, Belpani, B-Gaun, Bhuihara, Bichawagaudi, Bijaura, Bijayanagar, Bijuliya, Bishalnagar, Chauraha, Boradandi, C-Gaun, Chapartala, Chatakpur, Chaukidanda, Chunepani, Deurali, Devhariya, Devhariyachok, Devipur, D-Gaun, Dhadkuwa, Geti, Ghalghaletol, Ghodsuwa, Ghuinyanghat, Godawari, Haraiya, Hasanpur, Jai,Jamunabhadi, Jhalari, Jhallari, Jokaiya, Jonapur, Joralkatan, Jugeda, Jugedakatan, Kadigaun, Kailaligaun, Kankauwa, Khairana, Khairenikatan, Khallamauriphata, Khamaura, Kudasinkatan, Laksminagar, Lalpur, Loharpatti, Majgaukatan, Majgaun, Malakheti, Malakhetibajar, Manehara, Maneharagaudi, Mataiyakatan, Matiyari, Patela, Mauriphata, Mohanpur, Nawadiptol, Olani (Pokhariplat), Pathari, Phakalpur, Pipariya, Pokhrelkatan, Punarbasbasti, Raikawarbichawa, Rajpur, SantositolShivatalbasti, Shrilanka, Shripur, Simadikatan (Olanisimalkot), Sodandi, Swarkatan (Olani) Syaulibajar, Taranagar, Teghari, Tribenichok, Urmagoth, Urmi, Uttarpurwa

Table 4
Contribution of environmental factors.

S.N.	Environment variables	Contribution (%)
1	River Distance	33.1
2	LULC	30.3
3	DEM	11.9
4	Drainage density	10.6
5	Soil type	9.3
6	Annual temperature	2
7	TWI (Topographic Wetness Index)	1.8
8	Slope	0.5
9	NDVI	0.3
10	Annual precipitation	0

et al. (2013, 2015a, 2015b) in Malaysia, and Rahmati et al. (2016b) in the Golastan Province, Iran where these studies employed different models to conduct flood risk mapping. Regions situated near rivers are at an elevated vulnerability to flooding owing to heightened flood susceptibility (Fig. 6).

Furthermore, Li et al. (2019) discovered in global fourth-level watersheds that lower places with low elevation are more susceptible to damage, which is similar to our findings (Fig. 8). The elevated flow concentration in areas adjacent to the stream network significantly amplifies the likelihood of flooding occurrences (Glenn et al., 2012). The flood susceptibility was higher in shrubs than in other land covers (Fig. 7) which contrasts with prior studies i.e. Sugianto et al. (2022) and Zhang et al. (2018) which reported shrubs as an important land cover in controlling river discharge. The flood magnitudes exhibited a decline in regions characterized by higher elevations (Fig. 8). The response curves for elevation confirm this finding, showing that low-lying areas and plains are particularly vulnerable to flooding (Javidan et al., 2021). In areas with lower elevations, a significant volume of water goes into the stream network, leading to the flood incident (Lee et al., 2017). The findings of this study also concur with Dang and &Nguyen (2018) and Mashao et al. (2023) studies in the Lam River basin, Vietnam, and the east coast of South Africa respectively, which indicated that greater drainage densities led to an augmented flow of runoff, which is directly linked to a heightened susceptibility of flooding.

Moreover, Kalédjé et al. (2019) revealed that the higher the drainage density of a specific region, the more likely to be flooded which justifies its major influence on flood occurrence in Batouri (East Cameroon). The drainage pattern of an area can be influenced due to various factors like steepness of slopes, the rate at which water infiltrates the ground, the condition of vegetation cover, the characteristics of the soil structure and composition, and the geological formation (Pourtaghi and Pourghasemi, 2014). Haplaquents, Haplaqepts, and Eutrocrepts soil types are dominant in Terai and Inner Terai region (Gurung, 2020) which indicates high flood susceptibility in Terai (Fig. 10). Furthermore, the flood
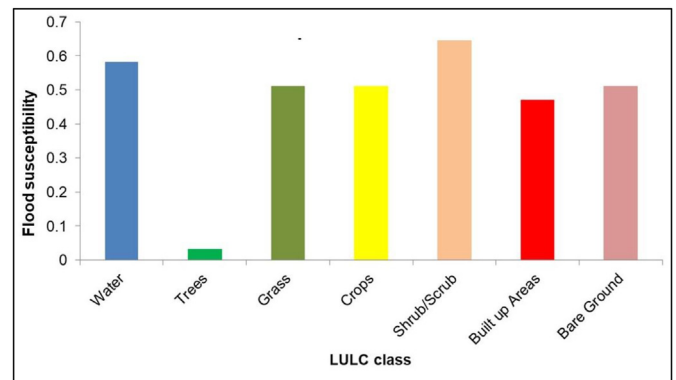
Fig. 7. LULC response to flood susceptibility.

susceptibility increased with rising temperature (Fig. 11). Because temperature is closely related to precipitation, elevated temperatures (beyond 24-degree Celsius) lead to increased rainfall due to precipitation triggered by local evapotranspiration and, as a result, increased flood susceptibility (Tabari, 2020).

The flood susceptibility was high at TWI value 5 and then decreased as TWI increased (Fig. 12). Similar trend was observed by Riadi et al. (2018) in Karawang regency in West Java Province in Indonesia which described a surge in flood susceptibility at TWI value > 25 and then decreased as TWI increased. However, our study's findings differ from Shreevastav et al. (2022) regarding the TWI trend in the southern Bagmati corridor of Nepal which reported a low flood risk until a TWI value of 15. Our study showed an inverse relationship beyond that threshold (Fig. 12). Furthermore, Das (2019) reported higher the TWI value the more floodable the area in the Ulhas basin, India. There may be certain regions with a high flood hazard level based on the flood hazard zones identified by TWI map analysis through TWI map analysis, particularly in regions with a history of past flood incidents (Riadi et al., 2018).

NDVI also has an impact on flood occurrence (rise and fall) (Fig. 13) which is similar to the finding by Askar et al. (2022) in Iraq. NDVI outcomes demonstrated consistency with the findings of prior studies by Tehrany et al. (2017) in China and Khosravi et al. (2016) in Haraz Watershed, Iran which applied multivariate statistical methods i.e., Logistic Regression and other models for flood risk (Mind'je et al., 2019). In contrast, Mashao et al. (2023) in South Africa showed that NDVI has no relationship with flood risk. Moreover, the occurrence of floods was influenced by deforestation resulting from agricultural activities and infrastructure development, including roads, recreational areas, and clustered settlements, in areas identified as highly susceptible based on NDVI modeling (Shreevastav et al., 2022). The higher the NDVI value, more the green vegetation which lowers direct runoff and controls floods (Shreevastav et al., 2022).
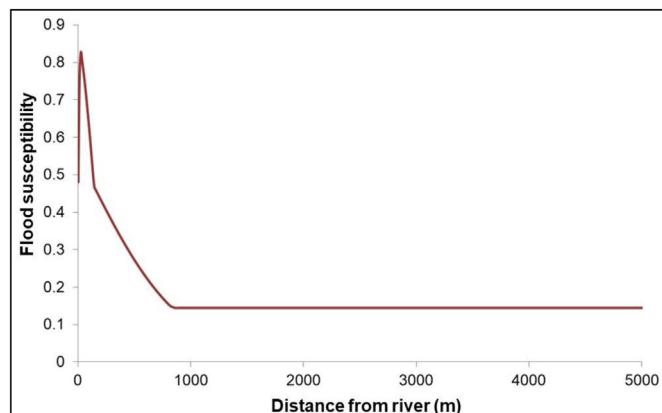
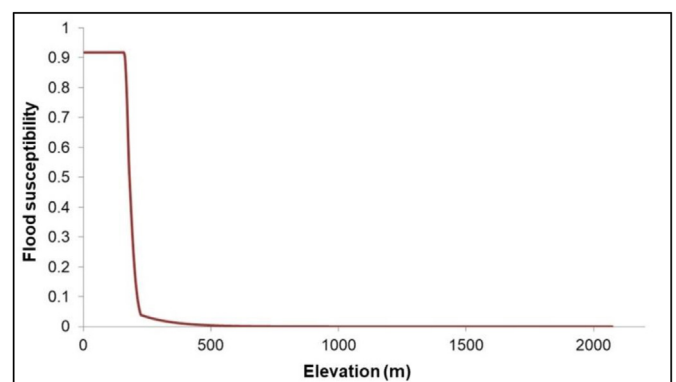**Fig. 6.** River distance response to flood susceptibility.

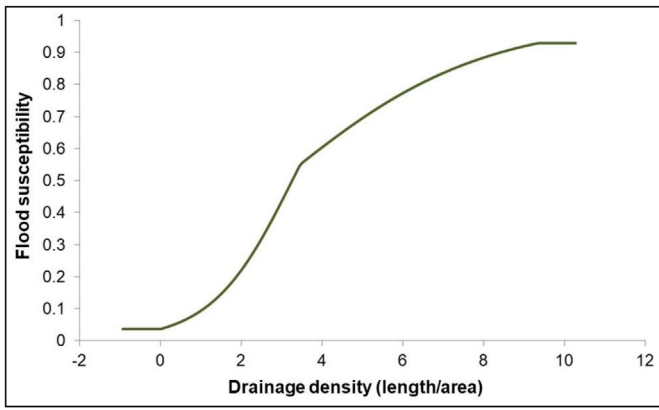**Fig. 8.** Flood susceptibility response to elevation.

Fig. 9. Flood susceptibility response to drainage density.
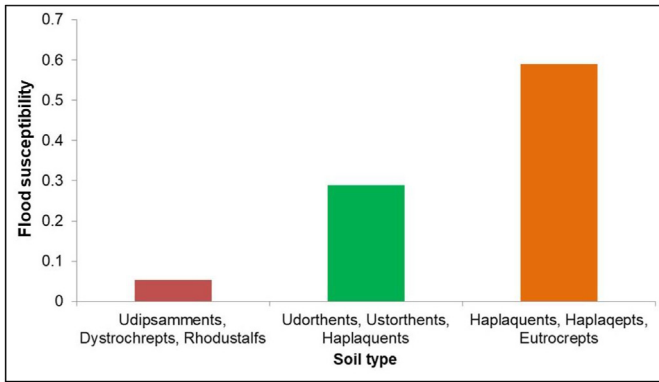

Fig. 10. Flood susceptibility response soil type.
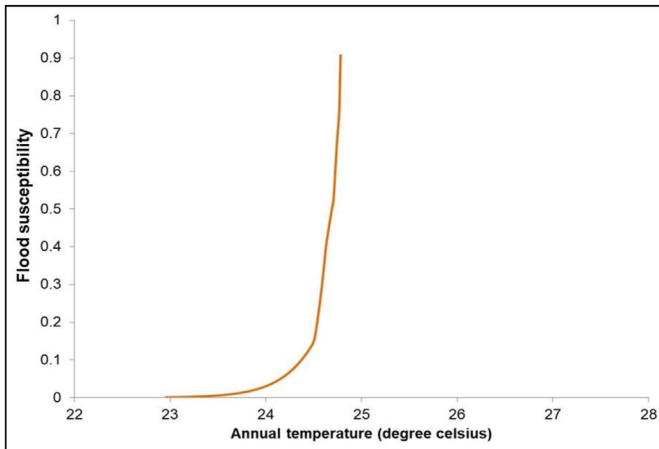

Fig. 11. Flood susceptibility response to annual temperature.
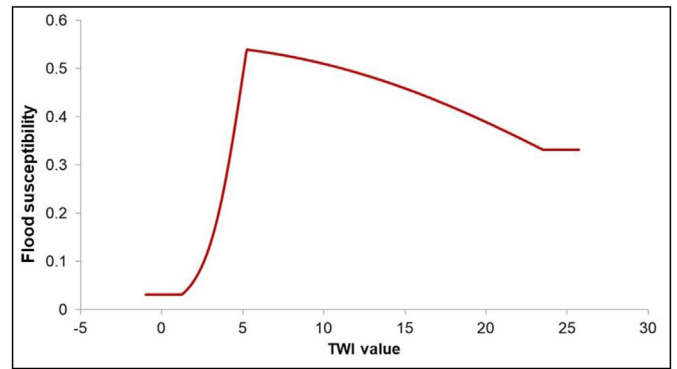

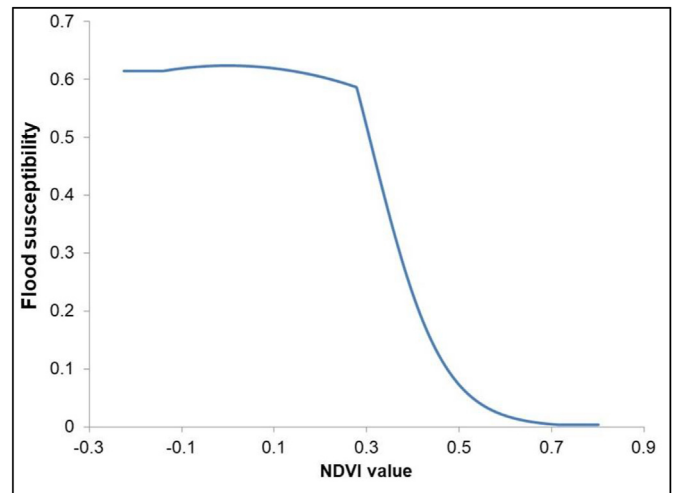**Fig. 12.** Flood susceptibility response to TWI.

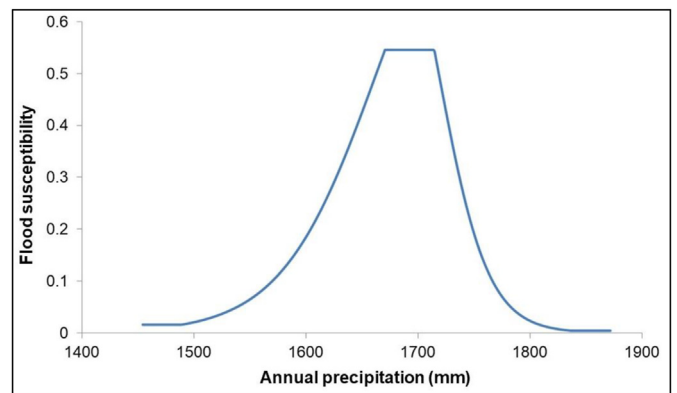**Fig. 13.** Flood susceptibility response to NDVI.

Fig. 14. Flood susceptibility response to annual precipitation.

The flood susceptibility remains constant till 1500 mm of annual precipitation (Fig. 14). However, Shreevastav et al. (2022) highlighted the constant flood risk up to 1400 mm of annual precipitation in the southern Bagmati corridor, Nepal. Blöschl et al. (2017) found that an increase in extreme precipitation resulted in greater flood discharges in Northwestern Europe. Prior studies in Germany (Schaller et al., 2014), USA (Risser and Wehner, 2017; Van Der Wiel et al., 2017), France (Philip et al., 2018), and Bangladesh (Philip et al., 2019) also stated precipitation/rainfall as the main causes of the flooding. On the other hand, intense rainfall in Dhaka (1988, 1998, 2004, 2007, 2015, 2016, 2017), along with other cities including Chittagong, Khulna, and Sylhet in Bangladesh leads to recurrent urban flooding and water logging issues (Dasgupta et al., 2015; Kabir et al., 2020). Pakistan has experienced recurring flooding in the years 2010, 2011, 2012, 2014, 2015, and 2017 due to heavy rainfall, while urban flooding is expected in major cities during the monsoon season (UNDRR, 2019; Shah et al., 2020).

Similarly, Colombo and its surrounding suburbs in Sri Lanka have experienced a notable surge in occurrences of flooding during the recent decades, and while the northern area of Kabul city, Afghanistan, has seen the emergence of urban flooding as a prominent problem during the monsoon season, marked by intense rainfall and insufficient drainage
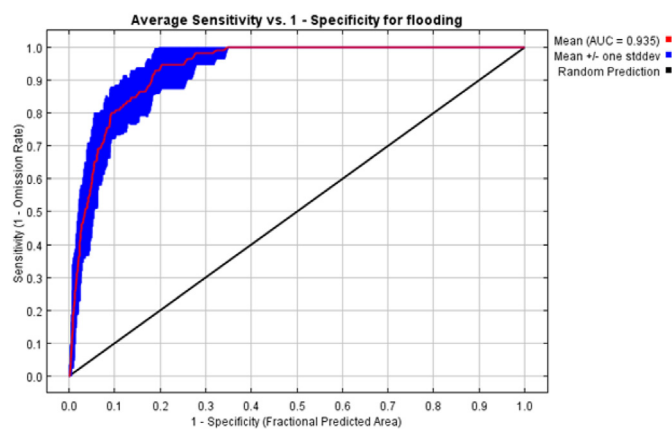
Fig. 15. AUC curve.

systems (Manawi et al., 2020; Manawadu and Wijeratne, 2021). A study by Duwal et al. (2023) showed that rainfall is considered a triggering factor for flooding and that increasing rainfall increases the possibility of flood incidences in Nepal's Karnali river basin. While a rise in precipitation typically amplifies the potential for floods (Shreevastav et al., 2022; Mashao et al., 2023), our findings reveal a contrary trend with a decrease in flood risk as precipitation levels increase (Fig. 14). Similar results reported by prior studies in the USA indicating that extreme precipitation alone might not be the most accurate predictor of flooding (Ivancic and Shaw, 2015; Mallakpour and Villarini, 2015; Berghuijs et al., 2016).

This is likely due to an increase in infiltration resulting from shallower freezing depths (Frolova et al., 2017). In general, more than mean rainfall, extreme rainfall rises with global mean surface temperature (Berg et al., 2013; Myhre et al., 2019), since the latter is constrained by evaporation, although extremes are also subject to alter due to localized in-storm processes. Simply put, more water vapor can be stored in warmer air and eventually fall as rain (Trenberth et al., 2003). In Clausius-Clapeyron scaling, the atmospheric water vapor capacity increases by approximately 6%–7% per degree of warming (Allan et al., 2014). More moisture in a warming environment can consequently result in more intense rainfall crises; this scale offers a first approximation (Fowler et al., 2021). As a result, this is incompatible with the idea that increases in intense rainfall (caused by temperature increases) will increase flood hazard globally (Blenkinsop et al., 2021). Furthermore, multiple studies have emphasized that factors like elevation, drainage density, and proximity to streams are the primary indicators closely linked to the susceptibility to incidents of floods (Convertino et al., 2014; Khosravi et al., 2016a,b; Bui et al., 2016).

4.3. Performance of MaxEnt model

The AUC depicting the MaxEnt model's performance is illustrated in Fig. 15. The flood points were arbitrarily divided into training (75%) and verification (25%) groups to develop and validate the model using the AUC methodology. The AUC demonstrated the model's performance of 79.8% performance rate (Mind'je et al., 2019), which is significantly lower than our study's performance. In this study, the AUC was determined to be 0.935, with a standard deviation of 0.018 (Fig. 15). Mashao et al. (2023) observed an AUC value of 0.899, which is somewhat less, and a standard deviation of 0.065, which is greater than our finding. However, this model's performance is lower than the study conducted by Javidan et al. (2021) at 97.2% but slightly higher than other studies i.e. 90% (Azare, 2021; Moradi et al., 2021), at 88.5% (DavoudiMoghaddam and Haghizadeh, 2020) and 76% (Darabi et al., 2020).

A study by Siahkamari et al. (2018) in the Madarsoo Watershed, Iran also found an AUC value of 92.6% which is close to our finding. A finding by Shreevastav et al. (2022) shows that the AUC value was 0.931 with a

standard deviation of 0.019 which is very near to our result value (Fig. 15). In the Golestan Province of Iran, AUC ranges between 0.933 and 0.936 for the floods using MaxEnt model (Javidan et al., 2021). Harshasimha and &Bhatt (2023) found an AUC value of 0.83 concerning the validation of flood inventory points in Assam, the northeastern part of India. Also, the model performance of our study i.e. 93.5% is lower than Norallahi and &SeyedKaboli (2021) at 98% and Eini et al. (2020) at 96.76% in Kermanshah City, Iran. The AUC is close to or greater than 0.8, indicating the accuracy of the MaxEnt model in estimating the spatial distribution of flood hazards at the province scale based on environmental factors (Mashao et al., 2023).

Nevertheless, the model is helpful and can be used for future flood susceptibility assessment due to excellent AUC i.e. 80%–90% (Mandrekar, 2010; Mashao et al., 2023). This study found that the model performs well for flood susceptibility mapping, with an AUC of 0.935 (Fig. 15). Park (2015) suggested the MaxEnt model as a powerful technique for managing continuous data, and its amalgamation with classified information showcases exceptional predictive capabilities. The significance of environmental factors can be used as a theoretical foundation for examining the risk of flash floods (Li et al., 2022).

5. Conclusion

We employed the MaxEnt machine learning approach to derive flood susceptibility maps for the Mohana-Khutiya River in Nepal. These maps not only aided in evaluating the flood susceptibility in each village but also enabled the identification of factors that significantly influence the susceptibility to flood in the Mohana-Khutiya River area. Our analysis revealed that the distance from the river (33.1%) and changes in LULC (30.3%) were the primary factors influencing flood susceptibility. Surprisingly, annual precipitation had negligible influence on flood susceptibility within the study area. Based on our results, we identified 20 villages in the high flood susceptible zone, followed by 45 villages in the moderate susceptible and 105 villages in the low susceptible zone. The high susceptible zone encompassed approximately 4.9% of the area, while the moderate-susceptible zone covered 12.75% and the low susceptible zone covered 82.34%.

The MaxEnt model, employed for spatial flood susceptible modeling in our study, yielded satisfactory results, as indicated by acceptable AUC values. Susceptibility mapping is crucial for preparing disaster management plans for local government, especially in flood-prone areas. MaxEnt modeling approach, noted for its cost-effectiveness, simplicity, and low data requirements, can be a fitting solution for developing countries like Nepal. By efficiently identifying vulnerable areas, MaxEnt contributes to proactive disaster planning, ultimately reducing the impact on property and lives. This study highlights the effectiveness of the MaxEnt model as a useful approach for academics and policymakers in understanding flood occurrences and aiding in flood mitigation planning and framework development.

Our findings also emphasize the importance of considering factors beyond annual precipitation when assessing flood susceptibility, underscoring the necessity for a holistic comprehension of variables such as distance from the river and LULC change. However, further research is necessary to strengthen this claim. Future research should focus on refining the MaxEnt model by incorporating additional variables and validating it against observed flood events. Additionally, exploring the integration of other flood modeling approaches or data sources could augment the precision and resilience of flood susceptible evaluations, which will be beneficial for developing effective disaster management plans.

Data statement

Data will be made available on request.

CRediT authorship contribution statement

Menuka Maharjan: Writing – review & editing, Writing – original draft, Supervision, Resources, Project administration, Conceptualization. **Sachin Timilsina:** Writing – review & editing, Writing – original draft, Data curation. **Santosh Ayer:** Writing – review & editing, Writing – original draft, Data curation. **Bikram Singh:** Validation, Software, Methodology, Formal analysis. **Bikram Manandhar:** Writing – review & editing, Methodology. **Amir Sedhain:** Writing – review & editing, Methodology.

Declaration of competing interest

The authors declare that they have no known competing financial interests or personal relationships that could have appeared to influence the work reported in this paper.

Acknowledgments

References

Abbas, A., Amjath-Babu, T.S., Kächele, H., Usman, M., Müller, K., 2016. An overview of flood mitigation strategy and research support in South Asia: implications for sustainable flood risk management. Int. J. Sustain. Dev. World Ecol. 23 (1), 98–111. https://doi.org/10.1080/13504509.2015.1111954.

ADB, 2020. Nepal: Priority River Basins Flood Risk Management Project (Mohana–Khutiya River), Initial Environmental Examination. Water Resources Project Preparatory Facility. Department of Water Resources and Irrigation for the Asian Development Bank.

Ahmadisharaf, E., Kalyanapu, A.J., Chung, E.S., 2016. Spatial probabilistic multi-criteria decision making for assessment of flood management alternatives. J. Hydrol. 533, 365–378. https://doi.org/10.1016/j.jhydrol.2015.12.031.

Allan, R.P., Liu, C., Zahn, M., Lavers, D.A., Koukouvagias, E., Bodas-Salcedo, A., 2014. Physically consistent responses of the global atmospheric hydrological cycle in models and observations. Surv. Geophys. 35, 533–552. https://doi.org/10.1007/s10712-012-9213-z.

Aldardasawi, A.F.M., Eren, B., 2021. Floods and their impact on the environment. Academic Perspective Procedia 4 (2), 42–49. https://doi.org/10.33793/acperpro.04.02.24.

Ali, S.A., Parvin, F., Pham, Q.B., Vojtek, M., Vojteková, J., Costache, R., et al., 2020. GIS-based comparative assessment of flood susceptibility mapping using hybrid multi-criteria decision-making approach, naïve Bayes tree, bivariate statistics, and logistic regression: a case of Topľa basin, Slovakia. Ecol. Indicat. 117, 106620.

Andaryani, S., Nourani, V., Haghighi, A.T., Keesstra, S., 2021. Integration of hard and soft supervised machine learning for flood susceptibility mapping. J. Environ. Manag. 291, 112731.

Antwi-Agyakwa, K.T., Afenyo, M.K., Angnuureng, D.B., 2023. Know to predict, forecast to warn: a review of flood risk prediction tools. Water 15 (3), 427.

Asian Development Bank (ADB), 2019. Nepal: Flood Risk Sector Assessment. https://www.adb.org/sites/default/files/project-documents/52014/52014-001-dpta-en.pdf. (Accessed 22 June 2023).

Asian Disaster Preparedness Center (ADPC), 2005. A Primer: Integrated Flood Risk Management in Asia. https://reliefweb.int/report/world/primer-integrated-flood-risk-management-asia. (Accessed 24 June 2023).

Askar, S., Zeraat Peyma, S., Yousef, M.M., Prodanova, N.A., Muda, I., Elsahabi, M., Hatamiafkoueieh, J., 2022. Flood susceptibility mapping using remote sensing and integration of decision table classifier and metaheuristic algorithms. Water 14 (19), 3062. https://doi.org/10.3390/w14193062.

Australian Institute Disaster Resilience (AIDR), 2022. Major Incidents Report 2021–22. https://www.aidr.org.au/media/9574/aidr_major-incidents-report_2021-22.pdf. (Accessed 25 May 2023).

Azare, A., 2021. Risk analysis of urban flood in Bandar Abbas using machine learning model and Analytic hierarchy process. Environmental Erosion Research Journal 11 (1), 36–57. https://doi.org/10.52547/jeer.11.1.36.

Baig, M.A., Xiong, D., Rahman, M., Islam, M.M., Elbeltagi, A., Yigez, B., Dewan, A., 2022. How do multiple kernel functions in machine learning algorithms improve precision in flood probability mapping? Nat. Hazards 113 (3), 1543–1562.

Bajracharya, S.R., Khanal, N.R., Nepal, P., Rai, S.K., Ghimire, P.K., Pradhan, N.S., 2021. Community assessment of flood risks and early warning system in Ratu Watershed, Koshi Basin, Nepal. Sustainability 13 (6), 3577.

Banstola, P., Krishna, P., Sapkota, B., 2019. Flood risk mapping and analysis using hydrodynamic model HEC-RAS: a case study of Daraudi River, Chhepatar, Gorkha, Nepal. J. Nat. Resour. 2 (3), 25–44. https://doi.org/10.33002/nr2581.6853.02033.

Barredo, J.I., 2007. Major flood disasters in Europe: 1950–2005. Nat. Hazards 42, 125–148. https://doi.org/10.1007/s11069-006-9065-2.

Berghuijs, W.R., Woods, R.A., Hutton, C.J., Sivapalan, M., 2016. Dominant flood-generating mechanisms across the United States. Geophys. Res. Lett. 43 (9), 4382–4390. https://doi.org/10.1002/2016GL068070.

Berg, P., Moseley, C., Haerter, J.O., 2013. Strong increase in convective precipitation in response to higher temperatures. Nat. Geosci. 6 (3), 181–185. https://doi.org/10.1038/ngeo1731.

Beshir, A.R., Mahato, M., Qamer, F.M., Shrestha, S., 2022. Managing Seeds and Agricultural Losses in the Wake of Extreme Climate Events: Lessons from Nepal. https://www.preventionweb.net/news/managing-seeds-and-agricultural-losses-wake-extreme-climate-events-lessons-nepal. (Accessed 21 November 2023).

Blenkinsop, S., Alves, L.M., Smith, A.J., 2021. Climate change increases extreme rainfall and the chance of floods. ScienceBrief 1–5. https://sciencebrief.org/uploads/reviews/ScienceBrief_Review_RAINFALL_Jun2021.pdf.

Blöschl, G., Hall, J., Parajka, J., Perdigão, R.A.P., Merz, B., Arheimer, B., Aronica, G.T., Bilibashi, A., Bonacci, O., Borga, M., Čanjevac, I., Castellarin, A., Chirico, G.B., Claps, P., Fiala, K., Frolova, N., Gorbachova, L., Gül, A., Hannaford, J., Živković, N., 2017. Changing climate shifts the timing of European floods. Science 357 (6351), 588–590. https://doi.org/10.1126/science.aan2506.

Brunner, M.I., Slater, L., Tallaksen, L.M., Clark, M., 2021. Challenges in modeling and predicting floods and droughts: a review. Wiley Interdisciplinary Reviews Water 8 (3), e1520. https://doi.org/10.1002/wat2.1520.

Bui, D.T., Pradhan, B., Nampak, H., Bui, Q.T., Tran, Q.A., Nguyen, Q.P., 2016. Hybrid artificial intelligence approach based on neural fuzzy inference model and metaheuristic optimization for flood susceptibility modeling in a high-frequency tropical cyclone area using GIS. J. Hydrol. 540, 317–330. https://doi.org/10.1016/j.jhydrol.2016.06.027.

Convertino, M., Muñoz-Carpena, R., Chu-Agor, M.L., Kiker, G.A., Linkov, I., 2014. Untangling drivers of species distributions: global sensitivity and uncertainty analyses of MaxEnt. Environ. Model. Software 51, 296–309. https://doi.org/10.1016/j.envsoft.2013.10.001.

Costache, R., Hong, H., Pham, Q.B., 2020. Comparative assessment of the flash-flood potential within small mountain catchments using bivariate statistics and their novel hybrid integration with machine learning models. Sci. Total Environ. 711, 134514.

Dang, M.T., Nguyen, D.B., 2018. Application of GIS technology to establish a drainage density hierarchical map for flood hazard zoning in the Lam River basin. Journal of Mining and Earth Science 59 (6), 32–42.

Darabi, H., Haghighi, A.T., Mohamadi, M.A., Rashidpour, M., Ziegler, A.D., Hekmatzadeh, A.A., Kløve, B., 2020. Urban flood risk mapping using data-driven geospatial techniques for a flood-prone case area in Iran. Nord. Hydrol 51 (1), 127–142. https://doi.org/10.2166/nh.2019.090.

Das, S., 2019. Geospatial mapping of flood risk and hydro-geomorphic response to the floods in Ulhas basin, India. Remote Sens. Appl.: Society and Environment 14, 60–74. https://doi.org/10.1016/j.rsase.2019.02.006.

Das, S., Gupta, A., 2021. Multi-criteria decision-based geospatial mapping of flood risk and temporal hydro-geomorphic changes in the Subarnarekha basin, India. Geosci. Front. 12 (5), 101206. https://doi.org/10.1016/j.gsf.2021.101206.

Dasgupta, S., Zaman, A., Roy, S., Huq, M., Jahan, S., Nishat, A., 2015. Urban Flooding of Greater Dhaka in a Changing Climate: Building Local Resilience to Disaster Risk. World Bank Publications. https://doi.org/10.1596/978-1-4648-0710-7.

DavoudiMoghaddam, D., Haghizadeh, A., 2020. Detection of susceptible areas to flooding and its most important contributing factors using the maximum entropy model in the Tashan watershed, Khuzestan. Watershed Management Research Journal 33 (4), 94–109. https://doi.org/10.22092/wmej.2020.341563.1307.

de Brito, M.M., Almoradie, A., Evers, M., 2019. Spatially-explicit sensitivity and uncertainty analysis in an MCDA-based flood vulnerability model. Int. J. Geogr. Inf. Sci. 33 (9), 1788–1806.

Dewan, T.H., 2015. Societal impacts and vulnerability to floods in Bangladesh and Nepal. Weather Clim. Extrem. 7, 36–42. https://doi.org/10.1016/j.wace.2014.11.001.

Dhakal, B.B., 2020. Flood Inundation Mapping of Kankai River Basin, Nepal [Master's Thesis]. Central Department of Hydrology and Meteorology, Tribhuvan University. https://elibrary.tucl.edu.np/bitstream/123456789/16478/1/All%20thesis.pdf.

Dodangeh, E., Singh, V.P., Pham, B.T., Yin, J., Yang, G., Mosavi, A., 2020. Flood frequency analysis of interconnected rivers by copulas. Water Resour. Manag. 34, 3533–3549.

Dung, N.B., Long, N.Q., Goyal, R., An, D.T., Minh, D.T., 2022. The role of factors affecting flood hazard zoning using analytical hierarchy process: a review. Earth Systems and Environment 6 (3), 697–713.

Duwal, S., Liu, D., Pradhan, P.M., 2023. Flood susceptibility modeling of the Karnali river basin of Nepal using different machine learning approaches. Geomatics, Nat. Hazards Risk 14 (1), 2217321. https://doi.org/10.1080/19475705.2023.2217321.

Eini, M., Kaboli, H.S., Rashidian, M., Hedayat, H., 2020. Hazard and vulnerability in urban flood risk mapping: machine learning techniques and considering the role of urban districts. Int. J. Disaster Risk Reduc. 50, 101687. https://doi.org/10.1016/j.ijdrr.2020.101687.

EmDAT, 2019. The CRED/OFDA International disaster Database. https://www.emdat.be/. (Accessed 12 December 2021).

Erena, S.H., Worku, H., 2018. Flood risk analysis: causes and landscape based mitigation strategies in Dire Dawa city, Ethiopia. Geoenvironmental Disasters 5 (1), 1–19. https://doi.org/10.1186/s40677-018-0110-8.

European floods, 2021. Germany Floods: Dozens Killed after Record Rain in Germany and Belgium. https://www.bbc.com/news/world-europe-57846200. (Accessed 14 May 2023).

Fowler, H.J., Lenderink, G., Prein, A.F., Westra, S., Allan, R.P., Ban, N., et al., 2021. Anthropogenic intensification of short-duration rainfall extremes. Nat. Rev. Earth Environ. 2 (2), 107–122. https://doi.org/10.1038/s43017-020-00128-6.

Frolova, N.L., Kireeva, M.B., Magrickiy, D.V., Bologov, M.B., Kopylov, V.N., Hall, J., Semenov, V.A., Kosolapov, A.E., Dorozhkin, E.V., Korobkina, E.A., Rets, E.P., Akutina, Y., Djamalov, R.G., Efremova, N.A., Sazonov, A.A., Agafonova, S.A., Belyakova, P.A., 2017. Hydrological hazards in Russia: Origin, classification, changes, and risk assessment. Nat. Hazards 88, 103–131. https://doi.org/10.1007/s11069-016-2632-2.

Fu, M., Fan, T., Ding, Z.A., Salih, S.Q., Al-Ansari, N., Yaseen, Z.M., 2020. Deep learning data-intelligence model based on adjusted forecasting window scale: application in daily streamflow simulation. IEEE Access 8, 32632–32651.

Ghapar, A.A., Yussof, S., Bakar, A.A., 2018. Internet of Things (IoT) architecture for flood data management. International Journal of Future Generation Communication and Networking 11 (1), 55–62. https://doi.org/10.14257/ijfgcn.2018.11.1.06.

Ghatak, M., Kamal, A., Mishra, O.P., 2012. Background paper flood risk management in South Asia. In: Proceedings of the SAARC Workshop on Flood Risk Management in South Asia, pp. 9–10.

Ghosh, S., Saha, S., Bera, B., 2022. Flood susceptibility zonation using advanced ensemble machine learning models within Himalayan foreland basin. Natural Hazards Research 2 (4), 363–374.

Glago, F.J., 2021. Flood disaster hazards; causes, impacts, and management: a state-of-the-art review. In: NoroozinejadFarsangi, Ehsan (Ed.), Natural Hazards-Impacts, Adjustments and Resilience, pp. 29–37. https://doi.org/10.3126/gjn.v15i01.42889.

Glenn, E.P., Morino, K., Nagler, P.L., Murray, R.S., Pearlstein, S., Hultine, K.R., 2012. Roles of salt cedar (Tamarix spp.) and capillary rise in salinizing a non-flooding terrace on a flow-regulated desert river. J. Arid Environ. 79, 56–65. https://doi.org/10.1016/j.jaridenv.2011.11.025.

Global Natural Disaster Assessment Report, 2022. Global Natural Disaster Profile for 2021. https://reliefweb.int/report/world/2021-global-natural-disaster-assessment-report. (Accessed 15 May 2023).

Gurung, S.B., 2020. Soil distribution in Nepal. NUTA Journal 7 (1–2), 79–89. https://doi.org/10.3126/nutaj.v7i1-2.39936.

Hallegatte, S., 2009. Strategies to adapt to an uncertain climate change. Global Environ. Change 19 (2), 240–247. https://doi.org/10.1016/j.gloenvcha.2008.12.003.

Hammami, S., Zouhri, L., Souissi, D., Souei, A., Zghibi, A., Marzougui, A., Dlala, M., 2019. Application of the GIS-based multi-criteria decision analysis and analytical hierarchy process (AHP) in the flood risk mapping (Tunisia). Arabian J. Geosci. 12, 1–16. https://doi.org/10.1007/s12517-019-4754-9.

Harshasimha, A.C., Bhatt, C.M., 2023. Flood vulnerability mapping using MaxEnt machine learning and analytical hierarchy process (AHP) of Kamrup metropolitan district, Assam. Environmental Sciences Proceedings 25 (1), 73. https://doi.org/10.3390/ECWS-7-14301.

IFRC, 2020. South Asia Floods: 9.6 Million People Swamped as Humanitarian Crisis Deepens. https://reliefweb.int/report/bangladesh/south-asia-floods-96-million-people-swamped-humanitarian-crisis-deepens. (Accessed 30 April 2023).

Internal Displacement Monitoring Centre (IDMC), 2020. Global Report on Internal Displacement 2020 (GRID 2020). https://www.internal-displacement.org/global-report/grid2020. (Accessed 25 April 2023).

Internal Displacement Monitoring Centre (IDMC), 2023. Global Report on Internal Displacement 2023 (GRID 2023). https://www.internal-displacement.org/sites/default/files/publications/documents/IDMC_GRID_2023_Global_Report_on_Internal_Displacement_LR.pdf. (Accessed 25 April 2023).

Ivancic, T.J., Shaw, S.B., 2015. Examining why trends in very heavy precipitation should not be mistaken for trends in very high river discharge. Climatic Change 133 (4), 681–693. https://doi.org/10.1007/s10584-015-1476-1.

Janizadeh, S., Avand, M., Jaafari, A., Phong, T.V., Bayat, M., Ahmadisharaf, E., Prakash, I., Pham, B.T., Lee, S., 2019. Prediction success of machine learning methods for flash flood risk mapping in the Tafresh watershed, Iran. Sustainability 11 (19), 5426. https://doi.org/10.3390/su11195426.

Javidan, N., Kavian, A., Pourghasemi, H.R., Conoscenti, C., Jafarian, Z., Rodrigo-Comino, J., 2021. Evaluation of multi-hazard map produced using MaxEnt machine learning technique. Sci. Rep. 11 (1), 6496. https://doi.org/10.1038/s41598-021-85862-7.

Jehanzaib, M., Ajmal, M., Achite, M., Kim, T.W., 2022. Comprehensive review: Advancements in rainfall-runoff modeling for flood mitigation. Climate 10 (10), 147. https://doi.org/10.3390/cli10100147.

Juned, F., 2022. Natural disaster and displacement in Assam: the case of floods and impact on marginalized communities. Rehabilitation 5, 8. https://sprf.in/wp-content/uploads/2022/09/DID-IB.pdf.

Kabir, M.H., Ahmed, I., Von Meding, J.V., Forino, G., Ghosh, A.K., 2020. Impacts of prolonged waterlogging on educational continuity at schools in peri-urban areas of Dhaka, Bangladesh. Dhaka University Journal of Earth and Environmental Sciences 9 (1), 13–23. https://doi.org/10.3329/dujees.v9i1.54857.

Kafle, K.R., Khanal, S.N., Dahal, R.K., 2017. Consequences of Koshi Flood 2008 in terms of sedimentation characteristics and agricultural practices. Geoenvironmental Disasters 4 (1), 1–13. https://doi.org/10.1186/s40677-017-0069-x.

Kalédjé, P.S.K., Ngoupayou, J.R.N., Takounjou, A.F., Zebsa, M., Rakotondrabe, F., Ondoa, J.M., 2019. Floods of 18 and 19 November 2016 in Batouri (East Cameroon): interpretation of the hydro-meteorological parameters and historical context of the post-event survey episode. Sci. World J. 2019. https://doi.org/10.1155/2019/3814962.

Kalyanapu, A.J., Judi, D.R., McPherson, T.N., Burian, S.J., 2012. Monte Carlo-based flood modeling framework for estimating probability-weighted flood risk. Journal of Flood Risk Management 5 (1), 37–48. https://doi.org/10.1111/j.1753-318X.2011.01123.x.

Karki, M., Khadka, D.B., 2020. Simulation of rainfall-runoff of Kankai River basin using SWAT model: a case study of Nepal. Int. J. Res. Appl. Sci. Eng. Technol. 8 (8), 308–326.

Karna, K.K., Nema, M.K., Khare, D., 2021. Application of HEC-HMS model for runoff simulation: a case study of Kankai River Basin in Nepal. Indian Water Resources Society 41 (2), 14–19.

Kazi, A., 2014. A review of the assessment and mitigation of floods in Sindh, Pakistan. Nat. Hazards 70 (1), 839–864. https://doi.org/10.1007/s11069-013-0850-4.

Khosravi, K., Nohani, E., Maroufinia, E., Pourghasemi, H.R., 2016a. A GIS-based flood susceptibility assessment and its mapping in Iran: a comparison between frequency ratio and weights-of-evidence bivariate statistical models with multi-criteria decision-making technique. Nat. Hazards 83, 947–987.

Khosravi, K., Pourghasemi, H.R., Chapi, K., Bahri, M., 2016b. Flash flood risk analysis and its mapping using different bivariate models in Iran: a comparison between Shannon's entropy, statistical index, and weighting factor models. Environ. Monit. Assess. 188 (12), 656. https://doi.org/10.1007/s10661-016-5665-9.

Kron, W., 2005. Flood risk= hazard• values• vulnerability. Water Int. 30 (1), 58–68. https://doi.org/10.1080/02508060508691837.

Lavé, J., Avouac, J.P., 2001. Fluvial incision and tectonic uplift across the Himalayas of central Nepal. J. Geophys. Res. Solid Earth 106 (B11), 26561–26591. https://doi.org/10.1029/2001JB000359.

Lee, J.Y., Kim, J.S., 2021. Detecting areas vulnerable to flooding using hydrological-topographic factors and logistic regression. Appl. Sci. 11 (12), 5652.

Lee, S., Kim, J.C., Jung, H.S., Lee, M.J., Lee, S., 2017. Spatial prediction of flood risk using random-forest and boosted-tree models in Seoul metropolitan city, Korea. Geomatics, Nat. Hazards Risk 8 (2), 1185–1203. https://doi.org/10.1080/19475705.2017.1308971.

Lehmkuhl, F., Schüttrumpf, H., Schwarzbauer, J., Brüll, C., Dietze, M., Letmathe, P., Völker, C., Hollert, H., 2022. Assessment of the 2021 summer flood in central Europe. Environ. Sci. Eur. 34 (1), 107. https://doi.org/10.1186/s12302-022-00685-1.

Li, X., Yan, D., Wang, K., Weng, B., Qin, T., Liu, S., 2019a. Flood risk assessment of global watersheds based on multiple machine learning models. Water 11 (8), 1654. https://doi.org/10.3390/w11081654.

Li, X., Yan, D., Wang, K., Weng, B., Qin, T., Liu, S., 2019b. Flood risk assessment of global watersheds based on multiple machine learning models. Water 11 (8), 1654.

Li, Y., Deng, X., Ji, P., Yang, Y., Jiang, W., Zhao, Z., 2022. Evaluation of landslide risk based on CF-SVM in nujiang prefecture. Int. J. Environ. Res. Publ. Health 19 (21), 14248. https://doi.org/10.3390/ijerph192114248.

Mallakpour, I., Villarini, G., 2015. The changing nature of flooding across the central United States. Nat. Clim. Change 5 (3), 250–254. https://doi.org/10.1038/nclimate2516.

Manawadu, L., Wijeratne, V.P.I.S., 2021. Anthropogenic drivers and impacts of urban flooding case study in Lower Kelani River Basin, Colombo Sri Lanka. Int. J. Disaster Risk Reduc. 57, 102076. https://doi.org/10.1016/j.ijdrr.2021.102076.

Manawi, S.M.A., Nasir, K.A.M., Shiru, M.S., Hotaki, S.F., Sediqi, M.N., 2020. Urban flooding in the northern part of Kabul City: causes and mitigation. Earth Systems and Environment 4 (3), 599–610. https://doi.org/10.1007/s41748-020-00165-7.

Mandrekar, J.N., 2010. Receiver operating characteristic curve in diagnostic test assessment. J. Thorac. Oncol. 5 (9), 1315–1316. https://doi.org/10.1097/JTO.0b013e3181ec173d.

Marsh, S., 2020. Nepal: Priority River Basins Flood Risk Management Project. The Philippines. https://policycommons.net/artifacts/403350/nepal/1372356/. (Accessed 22 August 2023). CID: 20.500.12592/pg6x3h.

Mashao, F.M., Mothapo, M.C., Munyai, R.B., Letsoalo, J.M., Mbokodo, I.L., Muofhe, T.P., Matsane, W., Chikoore, H., 2023. Extreme rainfall and flood risk prediction over the East Coast of South Africa. Water 15 (1), 50. https://doi.org/10.3390/w15010050.

Mehravar, S., Razavi-Termeh, S.V., Moghimi, A., Ranjgar, B., Foroughnia, F., Amani, M., 2023. Flood susceptibility mapping using multi-temporal SAR imagery and novel integration of nature-inspired algorithms into support vector regression. J. Hydrol. 617, 129100.

Mind'je, R., Li, L., Amanambu, A.C., Nahayo, L., Nsengiyumva, J.B., Gasirabo, A., Mindje, M., 2019. Flood risk modeling and hazard perception in Rwanda. Int. J. Disaster Risk Reduc. 38, 101211. https://doi.org/10.1016/j.ijdrr.2019.101211.

Mishra, A., Mukherjee, S., Merz, B., Singh, V.P., Wright, D.B., Villarini, G., Stedinger, J.R., 2022. An overview of flood concepts, challenges, and future directions. J. Hydrol. Eng. 27 (6), 03122001.

MOAD, 2021. Statistical Information on Nepalese Agriculture,2016/17. Ministry of Agricultural Development, Singh Durbar, Kathmandu.

Moradi, E., Rajabi, A., Shabanlou, S., Yosefvand, F., 2021. Identification of the most important environmental variables in spatial prediction of flood-prone areas using the maximum entropy model in parts of Golestan Province. Iran. J. Soil Water Res. 52, 899–915. https://doi.org/10.22059/IJSWR.2021.316143.668851.

Mosavi, A., Ozturk, P., Chau, K.W., 2018. Flood prediction using machine learning models: a literature review. Water 10 (11), 1536.

Most, H. van der, Marchand, M., 2017. Selecting measures and designing strategies for Integrated Flood Management - a guidance document. April, 46. www.wmo.int. (Accessed 25 April 2023). https://www.floodmanagement.info/publications/guidance%20-%20selecting%20measures%20and%20designing%20strategies_e_web.pdf.Retrived date.

Munawar, H.S., Hammad, A.W.A., Waller, S.T., 2021. A review of flood management technologies related to image processing and machine learning. Autom. ConStruct. 132, 103916. https://doi.org/10.1016/j.autcon.2021.103916.

Myhre, G., Alterskjær, K., Stjern, C.W., Hodnebrog, Ø., Marelle, L., Samset, B.H., et al., 2019. Frequency of extreme precipitation increases extensively with event rareness under global warming. Sci. Rep. 9 (1), 16063. https://doi.org/10.1038/s41598-019-52277-4.

Nachappa, T.G., Piralilou, S.T., Gholamnia, K., Ghorbanzadeh, O., Rahmati, O., Blaschke, T., 2020. Flood susceptibility mapping with machine learning, multi-criteria decision analysis and ensemble using Dempster Shafer Theory. J. Hydrol. 590, 125275.

Nakata, T., 1989. Active faults of the Himalayas of India and Nepal. Geol. Soc. Am. Spec. Pap. 232 (1), 243–264. https://doi.org/10.1130/SPE232-p243.

National Planning Commission (NPC), 2017. Nepal Flood 2017: Post Flood Recovery Needs Assessment. Government of Nepal, Kathmandu, Nepal. http://nra.gov.np/uploads/docs/jKT7cPkw6A171208105316.pdf.

Norallahi, M., SeyedKaboli, H., 2021. Urban flood hazard mapping using machine learning models: GARP, RF, MaxEnt, and NB. Nat. Hazards 106 (1), 119–137. https://doi.org/10.1007/s11069-020-04453-3.

OCHA, 2021. Asia and the Pacific: Weekly Regional Humanitarian Snapshot. https://reliefweb.int/report/afghanistan/asia-and-pacific-weekly-regional-humanitarian-snapshot-19-25-october-2021. (Accessed 15 May 2023).

OCHA, 2022. West and Central Africa flooding situation overview. https://reliefweb.int/report/democratic-republic-congo/west-and-central-africa-flooding-situation-overview. (Accessed 25 May 2023).

Ozkan, S.P., Tarhan, C., 2016. Detection of flood hazard in urban areas using GIS: Izmir case. Procedia Technology 22, 373–381. https://doi.org/10.1016/j.protcy.2016.01.026.

Papaioannou, G., Vasiliades, L., Loukas, A., 2015. Multi-criteria analysis framework for potential flood-prone areas mapping. Water Resour. Manag. 29 (2), 399–418. https://doi.org/10.1007/s11269-014-0817-6.

Parajuli, G., Neupane, S., Kunwar, S., Adhikari, R., Acharya, T.D., 2023. A GIS-based Evacuation Route planning in flood-susceptible area of Siraha Municipality, Nepal. ISPRS Int. J. Geo-Inf. 12 (7), 286.

Park, N.W., 2015. Using maximum entropy modeling for landslide risk mapping with multiple geoenvironmental data sets. Environ. Earth Sci. 73 (3), 937–949. https://doi.org/10.1007/s12665-014-3442-z.

Paudel, R.C., Basnet, K., Sherchan, B., 2019. Application of HEC-HMS model for runoff simulation: a case study of Marshyangdi river basin in Nepal. In: Proceedings of the IOE Graduate Conference, vol. 7, pp. 127–140 (Print).

Perera, D., Seidou, O., Agnihotri, J., Rasmy, M., Smakhtin, V., Coulibaly, P., Mehmood, H., 2019. Flood Early Warning Systems: A Review of Benefits, Challenges and Prospects. Report Series, Issue 08.UNU-INWEH, Hamilton. https://doi.org/10.13140/RG.2.2.28339.78880.

Philip, S., Kew, S.F., Jan van Oldenborgh, G., Aalbers, E., Vautard, R., Otto, F., Haustein, K., Habets, F., Singh, R., 2018. Validation of a rapid attribution of the May/June 2016 flood-inducing precipitation in France to climate change. J. Hydrometeor. 19 (11), 1881–1898. https://doi.org/10.1175/JHM-D-18-0074.1.

Philip, S., Sparrow, S., Kew, S.F., Van Der Wiel, K., Wanders, N., Singh, R., Hassan, A., Mohammed, K., Javid, H., Haustein, K., Otto, F.E.L., Hirpa, F., Rimi, R.H., Islam, A.K.M.S., Wallom, D.C.H., van Oldenborgh, G.J., 2019. Attributing the 2017 Bangladesh floods from meteorological and hydrological perspectives. Hydrol. Earth Syst. Sci. 23 (3), 1409–1429. https://doi.org/10.5194/hess-23-1409-2019.

Phillips, S.J., Anderson, R.P., Schapire, R.E., 2006. Maximum entropy modeling of species geographic distributions. Ecological modeling 190 (3–4), 231–259.

Pourtaghi, Z.S., Pourghasemi, H.R., 2014. GIS-based groundwater spring potential assessment and mapping in the Birjand Township, southern Khorasan Province, Iran. Hydrogeol. J. 22 (3), 643–662. https://doi.org/10.1007/s10040-013-1089-6.

Rahmati, O., Zeinivand, H., Besharat, M., 2016a. Flood hazard zoning in Yasooj region, Iran, using GIS and multi-criteria decision analysis. Geomatics, Nat. Hazards Risk 7 (3), 1000–1017. https://doi.org/10.1080/19475705.2015.1045043.

Rahmati, O., Pourghasemi, H.R., Zeinivand, H., 2016b. Flood risk mapping using frequency ratio and weights-of-evidence models in the Golastan Province, Iran. Geocarto Int. 31 (1), 42–70. https://doi.org/10.1080/10106049.2015.1041559.

Regmi, R.K., 2021. Sedimentation modeling of KarnaliChisapani multipurpose project reservoir, Nepal. J. Inst. Eng.: Series A 102 (3), 815–827. https://doi.org/10.1007/s40030-021-00550-z.

Rentschler, J., Salhab, M., Jafino, B.A., 2022. Flood exposure and poverty in 188 countries. Nat. Commun. 13 (1), 3527. https://doi.org/10.1038/s41467-022-30727-4.

Riadi, B., Barus, B., Yanuar, M.J.P., Pramudya, B., Pramudya, B., Pramudya, B., 2018, May. Identification and delineation of areas of flood hazard using high accuracy of DEM data. In: IOP Conference Series. *IOP Conference Series: Earth and Environmental Science*, vol. 149. IOP Publishing. https://doi.org/10.1088/1755-1315/149/1/012035.

Risser, M.D., Wehner, M.F., 2017. Attributable human-induced changes in the likelihood and magnitude of the observed extreme precipitation during Hurricane Harvey. Geophys. Res. Lett. 44 (24), 12–457. https://doi.org/10.1002/2017GL075888.

Rogers, D., Tsirkunov, V., 2011. Costs and benefits of early warning systems. Global assessment rep.The World Bank. https://www.preventionweb.net/english/hyogo/gar/2011/en/bgdocs/Rogers_&_Tsirkunov_2011.pdf.

Rosmadi, H.S., Ahmed, M.F., Mokhtar, M.B., Lim, C.K., 2023. Reviewing Challenges of Flood Risk Management in Malaysia. Water 15 (13), 2390.

Sahoo, S.N., Sreeja, P., 2015. Development of flood inundation maps and quantification of flood risk in an urban catchment of Brahmaputra River ASCE-ASME. J. Risk Uncertain Eng. Syst. 3, A4015001.

Sangroula, S., Adhikari, T.R., Parajuli, A., Poudyal, K., 2022. Impact of Climate Change on Future Flow Response in Marshyangdi River Basin, Nepal[Master's Thesis]. Central Department of Hydrology and Meteorology, Tribhuvan University. https://elibrary.tucl.edu.np/bitstream/123456789/14278/1/All%20Thesis.pdf.

Schaller, N., Otto, F.E.L., van Oldenborgh, G.J., Massey, N.R., Sparrow, S., Allen, M.R., 2014. The heavy precipitation event of may–June 2013 in the upper Danube and Elbe basins. Bull. Am. Meteorol. Soc. 95, S69–S72.

Schmidt, L., Heße, F., Attinger, S., Kumar, R., 2020. Challenges in applying machine learning models for hydrological inference: A case study for flooding events across Germany. Water resources research 56 (5) e2019WR025924.

Seydi, S.T., Kanani-Sadat, Y., Hasanlou, M., Sahraei, R., Chanussot, J., Amani, M., 2022. Comparison of machine learning algorithms for flood susceptibility mapping. Rem. Sens. 15 (1), 192.

Shah, A.A., Shaw, R., Ye, J., Abid, M., Amir, S.M., Pervez, A.K., Naz, S., 2019. Current capacities, preparedness, and needs of local institutions in dealing with disaster risk reduction in Khyber Pakhtunkhwa, Pakistan. Int. J. Disaster Risk Reduc. 34, 165–172.

Shah, S.M.H., Mustaffa, Z., Teo, F.Y., Imam, M.A.H., Yusof, K.W., Al-Qadami, E.H.H., 2020. A review of the flood hazard and risk management in the South Asian Region, particularly Pakistan. Scientific African 10, e00651. https://doi.org/10.1016/j.sciaf.2020.e00651.

Sharma, T.P.P., Zhang, J., Koju, U.A., Zhang, S., Bai, Y., Suwal, M.K., 2019. Review of flood disaster studies in Nepal: a remote sensing perspective. Int. J. Disaster Risk Reduc. 34, 18–27. https://doi.org/10.1016/j.ijdrr.2018.11.022.

Shreevastav, B.B., Tiwari, K.R., Mandal, R.A., Singh, B., 2022. Flood risk modeling in the southern Bagmati corridor, Nepal (a study from Sarlahi and Rautahat, Nepal). Progress in Disaster Science 16, 100260. https://doi.org/10.1016/j.pdisas.2022.100260.

Shrestha, B.R., Sapkota, L., Chidi, C.L., 2022. Flood risk mapping and analysis: a case study of Andheri Khola catchment, Sindhuli district, Nepal. Geographical Journal of Nepal 15 (1), 103–118. https://doi.org/10.3126/gjn.v15i01.42889.

Siahkamari, S., Haghizadeh, A., Zeinivand, H., Tahmasebipour, N., Rahmati, O., 2018. Spatial prediction of flood-susceptible areas using frequency ratio and maximum entropy models. Geocarto Int. 33 (9), 927–941. https://doi.org/10.1080/10106049.2017.1316780.

Sivakumar, S.S., 2015. Flood mitigation strategies adopted in Sri Lanka a review. Int. J. Sci. Eng. Res. 6 (2), 607–611. http://www.ijser.org.

Skilodimou, H.D., Bathrellos, G.D., Chousianitis, K., Youssef, A.M., Pradhan, B., 2019. Multi-hazard assessment modeling via multi-criteria analysis and GIS: a case study. Environ. Earth Sci. 78 (2), 1–21. https://doi.org/10.1007/s12665-018-8003-4.

Stöcklin, J., 2008. Developments in the geological exploration of Nepal. J. Nepal Geol. Soc. 38, 49–54.

Sugianto, S., Deli, A., Miswar, E., Rusdi, M., Irham, M., 2022. The effect of land use and land cover changes on flood occurrence in Teunom Watershed, Aceh Jaya. Land 11 (8), 1271. https://doi.org/10.3390/land11081271.

Tabari, H., 2020. Climate change's impact on floods and extreme precipitation increases with water availability. Sci. Rep. 10 (1), 13768. https://doi.org/10.1038/s41598-020-70816-2.

Tehrany, M.S., Pradhan, B., Jebur, M.N., 2013. Spatial prediction of flood susceptible areas using rule-based decision tree (DT) and a novel ensemble bivariate and multivariate statistical models in GIS. J. Hydrol. 504, 69–79. https://doi.org/10.1016/j.jhydrol.2013.09.034.

Tehrany, M.S., Pradhan, B., Jebur, M.N., 2014. Flood susceptibility mapping using a novel ensemble weights-of-evidence and support vector machine models in GIS. J. Hydrol. 512, 332–343.

Tehrany, M.S., Pradhan, B., Jebur, M.N., 2015a. Flood risk analysis and its verification using a novel ensemble support vector machine and frequency ratio method. Stoch. Environ. Res. Risk Assess. 29 (4), 1149–1165. https://doi.org/10.1007/s00477-015-1021-9.

Tehrany, M.S., Pradhan, B., Mansor, S., Ahmad, N., 2015b. Flood risk assessment using a GIS-based support vector machine model with different kernel types. Catena 125, 91–101. https://doi.org/10.1016/j.catena.2014.10.017.

Tehrany, M.S., Shabani, F., NeamahJebur, M., Hong, H., Chen, W., Xie, X., 2017. GIS-based spatial prediction of flood-prone areas using standalone frequency ratio, logistic regression, the weight of evidence, and their ensemble techniques. Geomatics, Nat. Hazards Risk 8 (2), 1538–1561. https://doi.org/10.1080/19475705.2017.1362038.

The Himalayan, 2022. Kailali, Kanchanpur Inundated. https://thehimalayantimes.com/environment/kailali-kanchanpur-inundated. (Accessed 20 November 2023).

Trenberth, K.E., Dai, A., Rasmussen, R.M., Parsons, D.B., 2003. The changing character of precipitation. Bull. Am. Meteorol. Soc. 84 (9), 1205–1218. https://doi.org/10.1175/BAMS-84-9-1205.

UNDRR, 2019. Disaster risk reduction in Pakistan: Status report 2019. UN Office for Disaster Risk Reduction. https://www.undrr.org/publication/disaster-risk-reduction-pakistan. (Accessed 25 May 2023).

UNICEF, 2022. Devastating Floods in Pakistan. https://www.unicef.org/emergencies/devastating-floods-pakistan-2022. (Accessed 25 May 2023).

Upreti, B.N., 1999. An overview of the stratigraphy and tectonics of the Nepal Himalaya. J. Asian Earth Sci. 17 (5–6), 577–606. https://doi.org/10.1016/S1367-9120(99)00047-4.

Van Der Wiel, K., Kapnick, S.B., Van Oldenborgh, G.J., Whan, K., Philip, S., Vecchi, G.A., Singh, R.K., Arrighi, J., Cullen, H., 2017. Rapid attribution of the August 2016 flood-

inducing extreme precipitation in south Louisiana to climate change. Hydrol. Earth Syst. Sci. 21 (2), 897–921. https://doi.org/10.5194/hess-21-897-2017.

Vojtek, M., Vojteková, J., 2019. Flood susceptibility mapping on a national scale in Slovakia using the analytical hierarchy process. Water 11, 364.

Wang, L., Cui, S., Li, Y., Huang, H., Manandhar, B., Nitivattananon, V., Fang, X., Huang, W., 2022. A review of the flood management: from flood control to flood resilience. Heliyon 8 (11), e11763. https://doi.org/10.1016/j.heliyon.2022.e11763.

Ye, Yuan, 2022. Officials "Deliberately" Hid Deaths during Henan Floods, Report Finds. https://www.sixthtone.com/news/1009524. (Accessed 15 May 2023).

Zeng, Z., Li, Y., Lan, J., Hamidi, A.R., 2021. Utilizing user-generated content and GIS for flood risk modeling in mountainous areas: a case study of Jian City in China. Sustainability 13 (12), 6929. https://doi.org/10.3390/su13126929.

Zhang, X., Lin, P., Chen, H., Yan, R., Zhang, J., Yu, Y., Liu, E., Yang, Y., Zhao, W., Lv, D., Lei, S., Liu, B., Yang, X., Li, Z., 2018. Understanding land use and cover change impacts on run-off and sediment load at flood events on the Loess Plateau, China. Hydrol. Process. 32 (4), 576–589. https://doi.org/10.1002/hyp.11444.